Sensors & Actuators: B. Chemical 367 (2022) 132030

Contents lists available at ScienceDirect

Sensors and Actuators: B. Chemical

journal homepage: www.elsevier.com/locate/snb

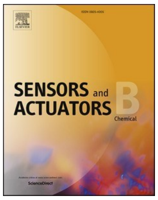

Gas sensing for industrial relevant nitrogen-containing compounds using a microelectronics-based absorption spectrometer in the 220–330 GHz frequency range

Timothy E. Rice [a], M. Arshad Zahangir Chowdhury [a], Megan N. Powers [a],
Muhammad Waleed Mansha [b], Ingrid Wilke [c], Mona M. Hella [b], Matthew A. Oehlschlaeger [a,*]

[a] Department of Mechanical, Aerospace, and Nuclear Engineering, Rensselaer Polytechnic Institute, United States
[b] Department of Electrical, Computer, and Systems Engineering, Rensselaer Polytechnic Institute, United States
[c] Department of Physics, Applied Physics, and Astronomy, Rensselaer Polytechnic Institute, United States

ARTICLE INFO

Keywords:
Gas sensing
Rotational spectroscopy
Terahertz
THz-wave
Nitrous oxide
Acetonitrile
Nitric acid
Nitromethane

ABSTRACT

Gas sensing for four nitrogen-containing compounds (nitrous oxide, acetonitrile, nitric acid, and nitromethane) is explored and demonstrated using rotational absorption spectroscopy carried out with a compact terahertz-wave microelectronics-based spectrometer operating in the 220–330 GHz frequency range. The four gases investigated are important in industrial processes, as well as in chemical, combustion, environmental, and agricultural contexts. Absorption measurements were made at room temperature (297 K) and moderate pressures (33.3–2133 Pa or 0.25–16 Torr) for the characterization of spectra that are comprised of distinct fingerprint features that include isolated single transitions and bands of pressure-broadened transitions, emanating from both ground vibrational states, as well as low-lying vibrationally-excited states. The measurements demonstrate that terahertz-wave quantitative gas sensing using all-electronic miniaturized systems is possible for nitrogen-containing compounds with detection limits of the order 10^{12}-10^{13} molecules cm^{-3} per meter pathlength and for dilute gases in air at 1 atm at concentrations of 5–1000 ppm per meter pathlength.

1. Introduction

Quantitative remote detection of gas-phase compounds in industrial and chemical processes is important for process and emissions monitoring and control. Nitrogen-containing compounds, such as nitrous oxide, acetonitrile, nitric acid, and nitromethane, are produced in large quantities for use in medical, energy, manufacturing, chemical, agricultural, and other applications. These nitrogen-containing compounds can also have deleterious impacts on the environment and human health; hence, remote gas sensing for these compounds during their manufacture, use, and in other industrial settings is desired.

Polar molecules, such as the nitrogen-containing compounds investigated here, have unique fingerprint rotational absorption spectra, offering the potential for the development of non-intrusive gas sensing technologies based on rotational absorption spectroscopy in the terahertz (THz) wave frequency range (0.1–10 THz) [1–8]. Absorption spectroscopy in THz-wave region can have advantages over the often-used infrared region, owing to the strong and selective absorption features polar molecules exhibit in this region and the absence of scattering by micron-sized airborne particles or aerosols at these frequencies [2]. Additionally, frequency ranges within the THz-wave can be selected that avoid water vapor absorption, that often interferes in remote gas sensing [9].

The advantages of THz-wave absorption spectroscopy, together with recent and rapid progress in microelectronics-based THz-wave sources and detectors [6,10–12], make possible the development of low-power and miniaturized systems for industrial and environmental remote gas sensing of polar molecules, including the four nitrogen-containing compounds investigated here, nitrous oxide, acetonitrile, nitric acid, and nitromethane.

In prior work, THz-wave gas sensing has been demonstrated for trace gas detection in human breath health diagnostics [13,14], cigarette smoke characterization [15], industrial and environmental volatile organic compound (VOC) detection [7,16], halogenated hydrocarbon detection [8], and other applications [17]. However, gas-phase THz-wave sensing for the four nitrogen-containing compounds

---

[*] Corresponding author.
E-mail address: oehlsm@rpi.edu (M.A. Oehlschlaeger).

https://doi.org/10.1016/j.snb.2022.132030
Received 29 March 2022; Received in revised form 6 May 2022; Accepted 10 May 2022

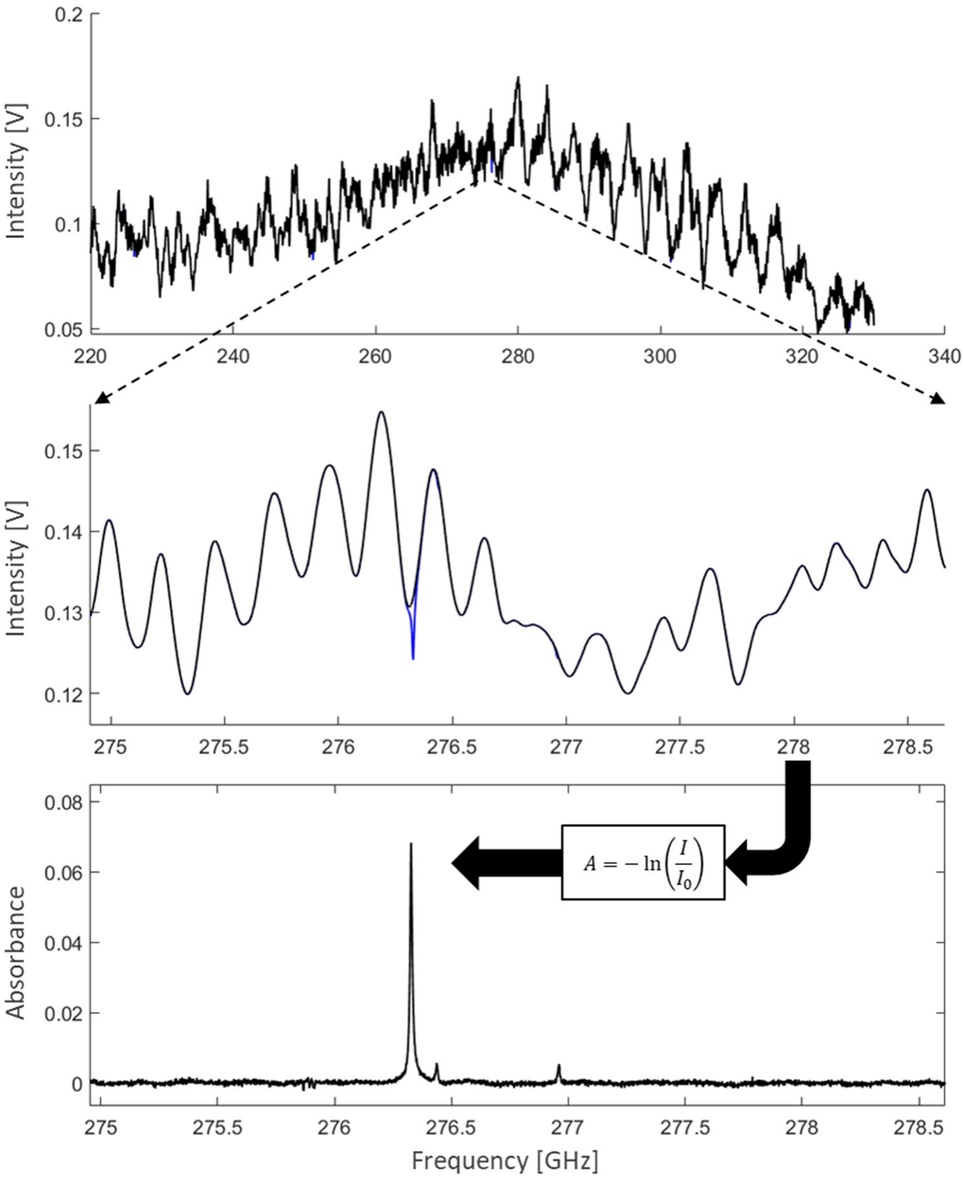

Fig. 1. Example experiment carried out for pure nitrous oxide at 133 Pa (1 Torr) and 297 K. Top and middle graphs: reference (I_0, black) and transmitted (I, blue) intensities as measured at the detector (top graph shows full frequency range and middle graph a subset); bottom graph: absorbance within a subset of the frequency range at 275–278.5 GHz.

investigated here is limited.

Nitrous oxide (N_2O) is a trace greenhouse gas found in the atmosphere that plays an important role in ozone depletion [18] and contributes significantly to global warming, owing to its strong radiative efficiency and relatively long atmospheric lifetime. It has a 100-year global warming potential (GWP) of 298 [19], relative to the GWP of carbon dioxide which is unity, and, hence, its production and emission control is of great importance. The majority of nitrous oxide atmospheric emissions come from agricultural soil management, which results in 75% of N_2O emission; while industrial, waste management, and transportation result in the remaining 25% [19]. Nitrous oxide is widely used as a medical anesthetic, a rocket propellant, in internal combustion engines, as a means of boosting power density of engines, and as an aerosol propellant. Due to its wide use and negative environmental consequences, remote gas sensing for industrial control of nitrous oxide emissions is desired.

Acetonitrile (CH_3CN, also known as methyl cyanide), is a by-product of several industrial and pharmaceutical processes, biomass burning, and is toxic to humans. Approximately 90% of atmospheric acetonitrile comes from biomass burning and high levels of acetonitrile in the atmosphere can be a good indicator of forest fires [20,21]. Moreover, due to its toxicity and use in industry, gas sensing for acetonitrile would be valuable in a number of environmental and human health applications.

Nitric acid (HNO_3) is a widely used chemical that has application in the manufacture of agricultural fertilizers, production of explosives, nylon, and other materials, and as an oxidant in a variety of industrial and chemical processes [22]. Nitric acid is also formed in the atmosphere from anthropogenic combustion and agricultural emissions and contributes to acid rain [23]. Owing to its wide use in industry and the negative consequence of nitric acid in the atmosphere, sensitive sensors for gas phase nitric acid are desired, such as explored here.

Nitromethane (CH_3NO_2) is the simplest organic nitro compound and is used as an industrial solvent and basic building block for organic synthesis reactions and other chemical processes. It is also used in dry cleaning, semiconductor manufacturing, and degreasing. Nitromethane is highly energetic and has long been used in explosives or fuels [24]. Gas-phase detection of this volatile and flammable compound could find several applications relating to chemical or industrial process control and emissions. Additionally, nitromethane has a strong dipole moment (3.5 Debye) [24], making it an ideal candidate detection via rotational absorption spectroscopy [24,25].

Here, we explore the potential for remote gas sensing using THz-wave rotational absorption spectroscopy for several nitrogen-containing compounds that are important in industrial or chemical processes. We demonstrate quantitative gas detection for nitrous oxide, acetonitrile, nitric acid, and nitromethane using a microelectronics-based source that provides high frequency resolution (0.5 MHz) and large bandwidth (220–330 GHz) suitable for miniaturized remote gas sensors.

2. Experimental methods

Absorption spectra in the 220–330 GHz frequency range were acquired using the hardware and methods developed in Rice et al. [7], where the experiment is comprised of a microelectronic source that applies 18 × frequency multiplication to a radio frequency input signal (VDi SGX, model WR 3.4 220–330 GHz, output power 0.25–0.6 mW) and that radiation is passed through a gas cell and its intensity monitored using a Schottky diode detector (VDi, model QOD 3–15). In prior work, we have carried out absorption measurements using amplitude modulation with lock-in detection. However, in this study, amplitude modulation was not used. Instead, direct absorption using unmodulated scanned-frequency radiation was implemented, which resulted in better frequency resolution (0.5 MHz) for rapid frequency sweep rates (160 GHz/s). To improve the signal-to-noise ratio, 40 successive frequency scans were averaged resulting in a total acquisition time of 27.5 s for each spectra.

The spectral absorption of gas samples was determined using the Beer-Lambert law:

$$A = \varepsilon c l = \ln\left(\frac{I}{I_0}\right),$$

where A is the absorbance, ε the absorption coefficient, c the concentration of the absorbing gas, l the pathlength, I the transmitted intensity of the radiation after absorption, and I_0 the reference intensity (no absorption). The absorption coefficient varies with frequency, temperature, pressure, and gas mixture composition, through the contribution of the line intensities and shapes for each transition. The gas cell pathlength, l, for the experiments conducted here was 21.6 cm.

To measure an absorption spectrum, we first record the reference intensity by sweeping the radiation source in frequency space while the gas cell is under vacuum. Next, the cell is filled with the gas of interest to a desired pressure, the radiation source is swept again in frequency, the transmitted intensity is recorded, and the Beer–Lambert law is applied to convert the measured intensities to absorbance. Successive absorption scans are averaged to improve the signal-to-noise ratio and the resulting absorption spectrum has a noise floor of ± 0.001 to ± 0.003 in absorbance and a frequency resolution of 0.5 MHz. Between experiments, the gas cell is purged of residual gases via several purge-vacuum cycles, where the gas cell is purged with pure N_2 gas and evacuated to 10^{-6} Torr.

An example experiment is shown in Fig. 1. Note, the strong low-frequency variation in the radiation intensity is due to standing waves that emanate from the parallel surfaces of the gas cell windows. These standing waves are minimized by the gas cell Brewster angle windows but not eliminated. For the most part, this low-frequency variation is cancelled from the absorbance using common-mode rejection (e.g., division of absorbed and reference signal in the Beer-Lambert law) and any remaining low-frequency noise results from subtle fluctuation in standing waves that occurs due to changes in the optical path that occurs between measurement of reference and absorbed intensity.

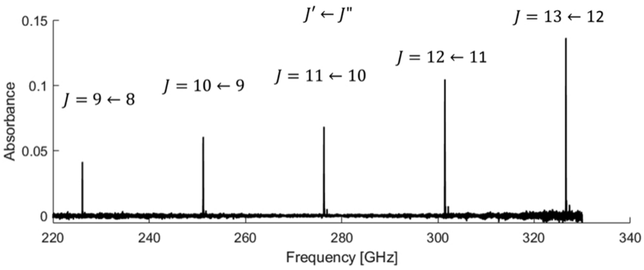

Fig. 2. Measured N_2O spectrum for 220–330 GHz (297 K and 133 Pa (1 Torr)). The strong rotational features are for transitions from the ground vibrational state.

3. Results and discussion

Measurements of spectral absorbance have been made in the 220–330 GHz frequency range for four nitrogen-containing gases of importance in industrial processes. Measurements were carried out at 297 K and the pressures from 33.3 to 2133 Pa (0.25–16 Torr). Reagent grade chemicals from Sigma-Aldrich with natural isotopic composition were used at purity levels of > 99%, with the exception of nitric acid, which was procured at 65% in water. Upon vaporization, the 65% aqueous nitric acid solution produces a gas phase mixture that is 26% nitric acid and 74% water vapor at 297 K [26]. In the present frequency range water vapor has negligible absorption at the concentrations encountered, with the exception of a weak feature at 325 GHz [7]. Example measurements of spectral absorbance are shown in the below figures within this section for experiments carried out at pressures of 267 Pa (2 Torr) or lower. Additional experimental results can be found in the appended supplementary materials.

Nitrous oxide (N_2O), a linear molecule, displays a simple absorption spectrum in the 220–330 GHz region, with five strong rotational transitions that emanate from the ground vibrational state and two weaker neighboring transitions for every strong transition that emanate from vibrationally excited states. The strong transitions are spaced at twice the ground state rotational constant, $2B$, where $B = 12.562$ GHz [27] and are located at frequencies of $2B(J'' + 1)$ for $J'' = 8$–12 and $J' = J'' + 1$, where J'' is the quantum number for total rotational angular momentum for the lower state and J' for the upper state.

For every strong N_2O transition, we observe two neighboring weak transitions for a vibrationally excited state where the lowest-energy degenerate bending mode of the linear N_2O is excited. These transitions also exist at frequencies of $2B(J'' + 1)$ for $J'' = 8$–12 and $J' = J'' + 1$ and correspond to the $(0\ 1^{1c}\ 0)$ bending-mode state with a rotational constant of $B = 12.567$ GHz and the $(0\ 1^{1d}\ 0)$ bending-mode state with a rotational constant of $B = 12.590$ GHz [27]. The measured N_2O transition frequencies agree with those documented in JPL molecular spectroscopy database [28] as shown in Figs. 2 and 3. Additionally, the reported relative line intensities from the JPL database agree well with the measurements as indicated by the line heights in Fig. 3.

Measured absorption spectra for acetonitrile (CH_3CN) are shown in Figs. 4 and 5. Acetonitrile is a symmetric top molecule with rotational constants of $A = 157.3$ GHz and $B = C = 9.199$ GHz [29]. The spectrum for a total pressure of 133 Pa (1 Torr) (Fig. 4) illustrates broad pressure-blended repeating absorption features that are spaced every $2B$ and centered at frequencies of $2B(J'' + 1)$. At a lower pressure of 33.3 Pa (0.25 Torr) (Fig. 5), the features are less blended and some of the underlying rotational structure reveals itself.

In Fig. 5, the transitions documented in the JPL molecular spectroscopy database [28] are superimposed on the experimental spectra, with each transition height representing a relative line intensity. It is observed that each blended feature is comprised of a series of transitions for different K values, the quantum number representing the projection

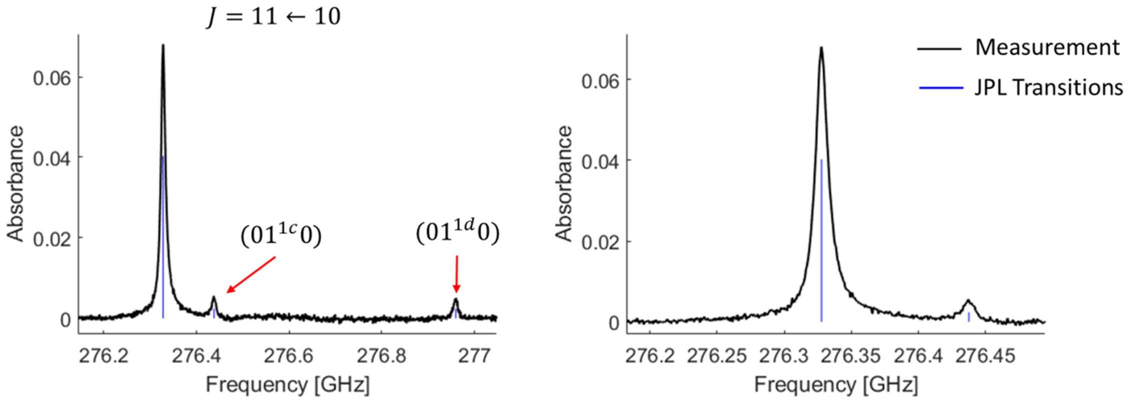

Fig. 3. Measured N_2O absorption (297 K and 133 Pa (1 Torr)) around $J'' = 10$ transitions, illustrating the strong ground state transition and two weaker vibrationally-excited (bending mode) transitions with comparison to JPL [28] transition frequency locations and relative line strengths.

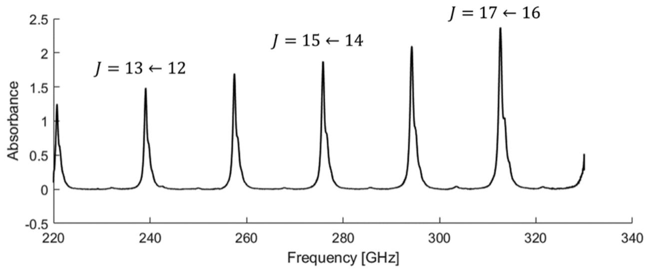

Fig. 4. Measured acetonitrile absorption spectrum for 220–330 GHz (297 K and 133 Pa (1 Torr)).

of total angular momentum onto the axis of symmetry. In this case the individual transitions follow selection rules of $J'' + 1 \leftarrow J''$, $\Delta K = 0$, and $K = 0$ to $K = J'' + 1$, and there is a decay in intensity with increasing K. In addition, to the ground vibrational state features (blue JPL lines), features are experimentally observed for a low-lying vibrationally-excited state, where these vibrationally-excited features (red JPL lines) exhibit the same shape as the ground-state features but are shifted to higher frequencies. The vibrationally-excited acetonitrile transitions occur for a lower state where the C-C-N bending mode is excited ($v_8 = 1$, energy of $\sim$362 cm^{-1}) [30].

Absorption measurements for nitric acid (HNO_3) are shown in Figs. 6–8 with the frequencies and relative strengths of transitions from the JPL database [28] shown in blue. Nitric acid was prepared in the gas phase from an aqueous nitric acid solution, creating a gas phase mixture that is 26% nitric acid and 74% water vapor [26]. However, water vapor only has a weak absorption feature at 325 GHz in the current frequency region at the partial pressures encountered in the present experiments [7]. Hence, at frequencies aside from 325 GHz, the current measurements illustrate most pure nitric acid absorption with water vapor serving as a collisional broadening partner.

The measured nitric acid absorption data agrees with the JPL predictions [28] for the frequency locations of transitions and their relative strengths. Nitric acid is a near-oblate asymmetric top molecule having rotational constants of $A = 13.011$ GHz, $B = 12.010$ GHz, and $C = 6.261$ GHz [31]. In the current frequency range, bands of rotational absorption lines are observed at frequencies spaced by 2 C, in keeping with R-branch c-type transitions with selection rules $\Delta J = +1$, $\Delta K_a = +1$, and $\Delta K_c = 0$, which describes the strongest transitions in the present frequency range. K_a and K_c are the quantum numbers for the

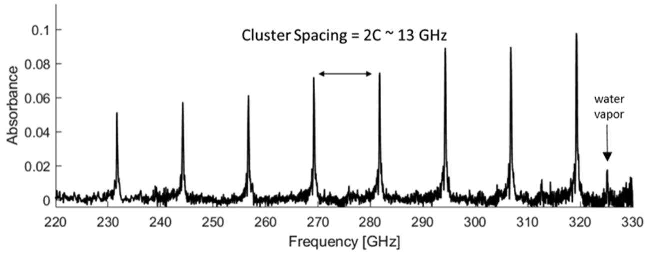

Fig. 6. Measured nitric acid absorption spectrum for 220–330 GHz (297 K and 69.3 Pa (0.52 Torr) nitric acid and 197 Pa (1.48 Torr) water vapor).

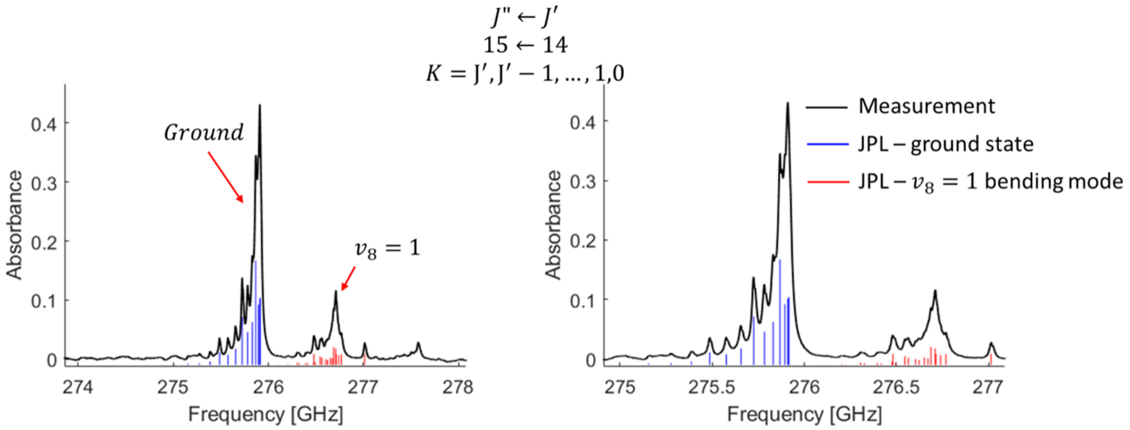

Fig. 5. Acetonitrile absorption (297 K and 33.3 Pa (0.25 Torr)) around $J'' = 14$ features, illustrating a series of strong ground state transitions (blue) and weaker vibrationally-excited transitions (red) with comparison to JPL [28] transition frequency locations and relative line strength.

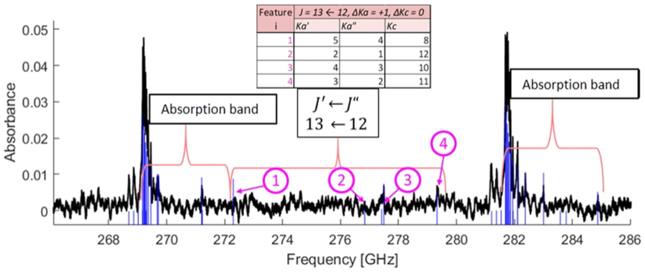

Feature i	$J = 13 \leftarrow 12, \Delta Ka = +1, \Delta Kc = 0$		
	Ka'	Ka"	Kc
1	5	4	8
2	2	1	12
3	4	3	10
4	3	2	11

Fig. 7. Measured nitric acid absorption spectrum for 267–286 GHz (297 K and 34.7 Pa (0.26 Torr) nitric acid and 98.7 Pa (0.74 Torr) water vapor, 133 Pa (1 Torr total)). Two absorption bands of *R*-branch *c*-type transitions are observed and compared to absorption lines and their relative strengths (blue) listed in the Jet Propulsion Laboratory (JPL) spectroscopic catalog [28].

projections of the total angular momentum onto the *a*- and *c*-axes. As shown in Fig. 8, each *R*-branch *c*-type absorption band is composed of a sequence of transitions. The absorption band is comprised of transitions described by: $J'_i = J'_1 - i + 1, K'_{a,i} = K'_{a,1} - 2(i - 1), K_{c,i} = K_{c,1} + i - 1$, where *i* indexes the transitions within a band.

Measured absorption spectra for nitromethane (CH_3NO_2) are illustrated in Figs. 9 and 10. Nitromethane is an asymmetric rotor with rotational constants of $A = 13.341$ GHz, $B = 10.545$ GHz, and $C = 5.876$ GHz [32]. Though nitromethane's rotational spectrum is slightly more complex than that of nitric acid, owing to its greater degree of asymmetry, its exhibits similar characteristics. In the case of nitromethane, strong absorption bands of *R*-branch *b*-type ($\Delta J = +1$, $\Delta K_a = \pm 1$, and $\Delta K_c = \pm 1$) and *c*-type ($\Delta J = +1$, $\Delta K_a = +1$, and $\Delta K_c = 0$) transitions spaced by $2C$ are observed. There are also weaker *Q*-branch transitions, described by $\Delta J = 0$, $\Delta K_a = 0$ and ± 1, and $\Delta K_c = 0$ and ± 1.

For nitromethane, fundamental spectroscopic data, including transition frequencies, is not available from JPL [28] or other databases for comparison, indicating the novelty and importance of the current nitromethane measurements. For comparison to the current measurements, we carried out spectral predictions for the ground state using the PGOPHER simulation code [33] and they are shown in Figs. 9 and 10. Note, that nitromethane has a low-lying vibrational mode at 470 cm^{-1} that at room temperature contains about 10% of the population and should contribute to the spectral absorption in the present frequency range, presumably at slightly higher shifted frequencies than the ground vibrational state. However, this vibrationally-excited state is not accounted for in the PGOPHER simulations, as the vibrationally-excited

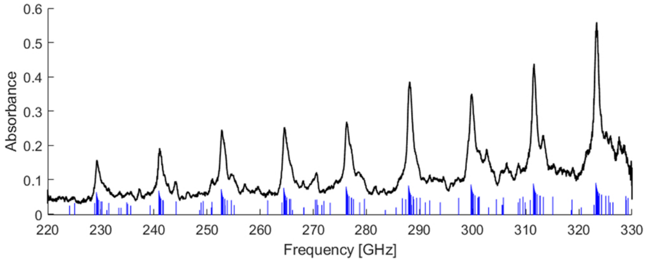

Fig. 9. Measured nitromethane absorption spectrum for 220–330 GHz (297 K and 133 Pa (1 Torr)).with comparison to PGOPHER [33] predicted transition locations and relative strengths.

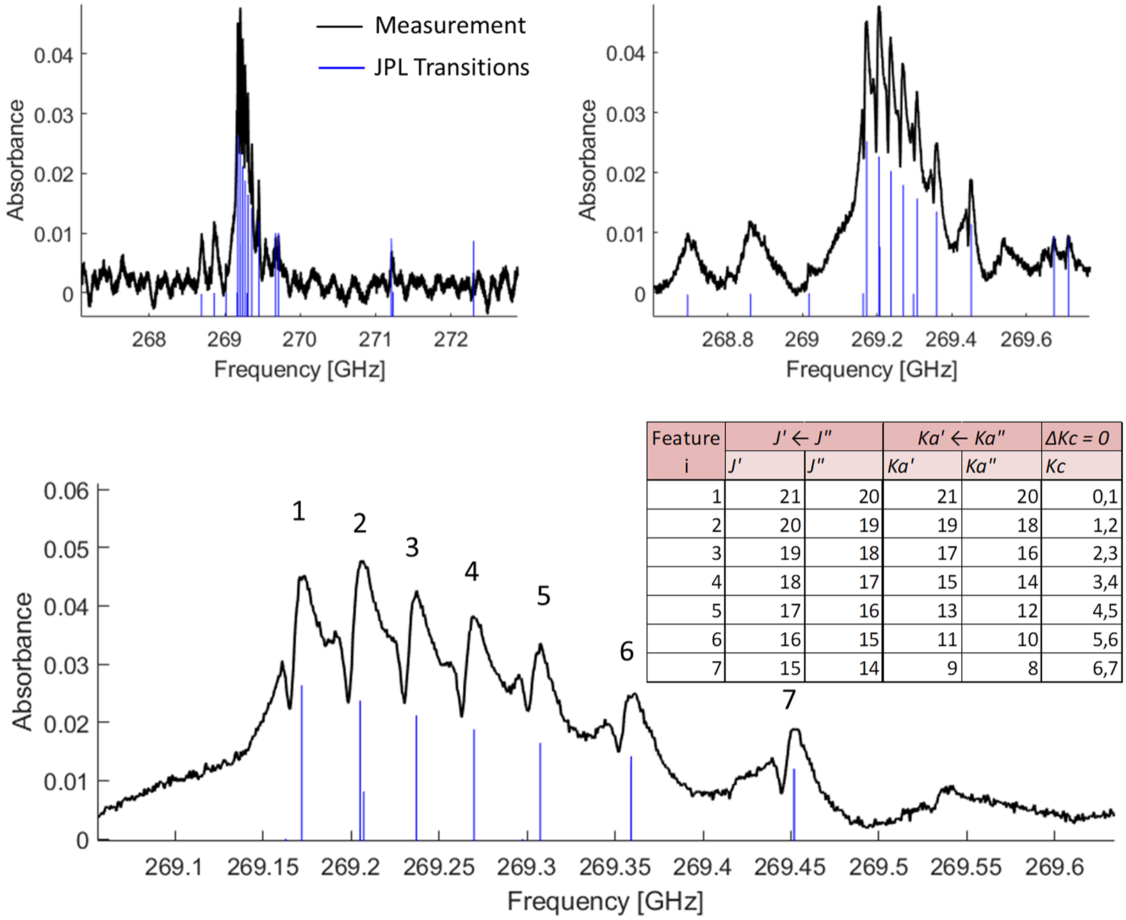

Feature i	J' ← J"		Ka' ← Ka"		ΔKc = 0
	J'	J"	Ka'	Ka"	Kc
1	21	20	21	20	0,1
2	20	19	19	18	1,2
3	19	18	17	16	2,3
4	18	17	15	14	3,4
5	17	16	13	12	4,5
6	16	15	11	10	5,6
7	15	14	9	8	6,7

Fig. 8. Measured nitric acid absorption spectrum (conditions of Fig. 7) with comparison to JPL transition locations and relative strengths (blue) [28].

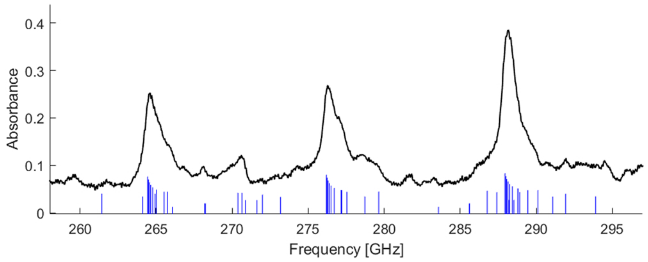

Fig. 10. Measured nitromethane absorption spectrum for 260–295 GHz (297 K and 133 Pa (1 Torr)) with comparison to PGOPHER [33] predicted transition locations and relative strengths.

rotational constants are not known.

Combined absorption spectra measurements in the 220–330 GHz range for the four compounds of interest, nitrous oxide, acetonitrile, nitric acid, and nitromethane, are shown in Fig. 11 with recommended frequencies for gas sensing at reduced pressures within the current range. The recommended frequencies were selected based upon potential interference from the other nitrogen-containing compounds and the strength of absorption at the selected frequencies. However, since the potential interference is a function of pressure, through line broadening effects, the optimal frequency for detection may vary depending on pressure and the presence of interfering species. These experiments illustrate the potential for THz gas sensing based on miniature silicon microelectronics sources, such as used in the present study, and demonstrate the sensitivity and selectivity of the sensing technique. As illustrated above, the sensor and technique is able to resolve relatively narrow spectral features (frequency resolution of 0.5 MHz), over a large bandwidth (220–330 GHz), and for reasonable frequency scanning rates (160 GHz/s). Such sensing capabilities allow for the analysis of gas mixtures, where the resulting absorption spectrum can be very complex.

Within the current frequency range, acetonitrile exhibits the strongest absorption, at all pressures, and sharp absorption features, making its selective and sensitive detection possible at many frequencies. We suggest the acetonitrile features at 239.096 and 294.251 GHz as the preferred frequencies for its detection, owing to the relative strength of acetonitrile absorption to the underlying nitromethane absorption at these frequencies. Nitromethane exhibits strong absorption and a broad underlying continuum spectrum. It is completely isolated from the absorption features of the other species at 287.942 and 323.196 GHz, at the pressures of the current study, making these frequencies ideal for its isolated detection.

The broad continuum exhibited by nitromethane, even at the modest pressures of the present study, makes the detection of the weaker absorbing nitrous oxide and nitric acid difficult in the presence of nitromethane. However, in the absence of nitromethane, isolated features for these two species at higher frequencies make their sensitive detection possible at pressures encountered in the current study. Within the current frequency range, nitrous oxide is best detected at 226.094 and 301.442 GHz, where it is isolated from acetonitrile and nitric acid. Nitric acid is best detected at 244.143 and 281.539 GHz, where it is isolated from acetonitrile and nitrous oxide, and can be detected in the

Table 1
Estimated detection limits at 297 K and 1 m pathlength.

Compound	Detection Frequencies [GHz]	Detection limit for pure gas [molecules cm^{-3}]	Detection limit for dilute gases in air at 1 atm [ppm]
Nitrous Oxide	226.094, 301.442	5.0×10^{13}	1000
Acetonitrile	239.096, 294.251	3.5×10^{12}	5
Nitric Acid	244.143, 281.539	3.7×10^{13}	20
Nitromethane	287.942, 323.196	1.4×10^{13}	20

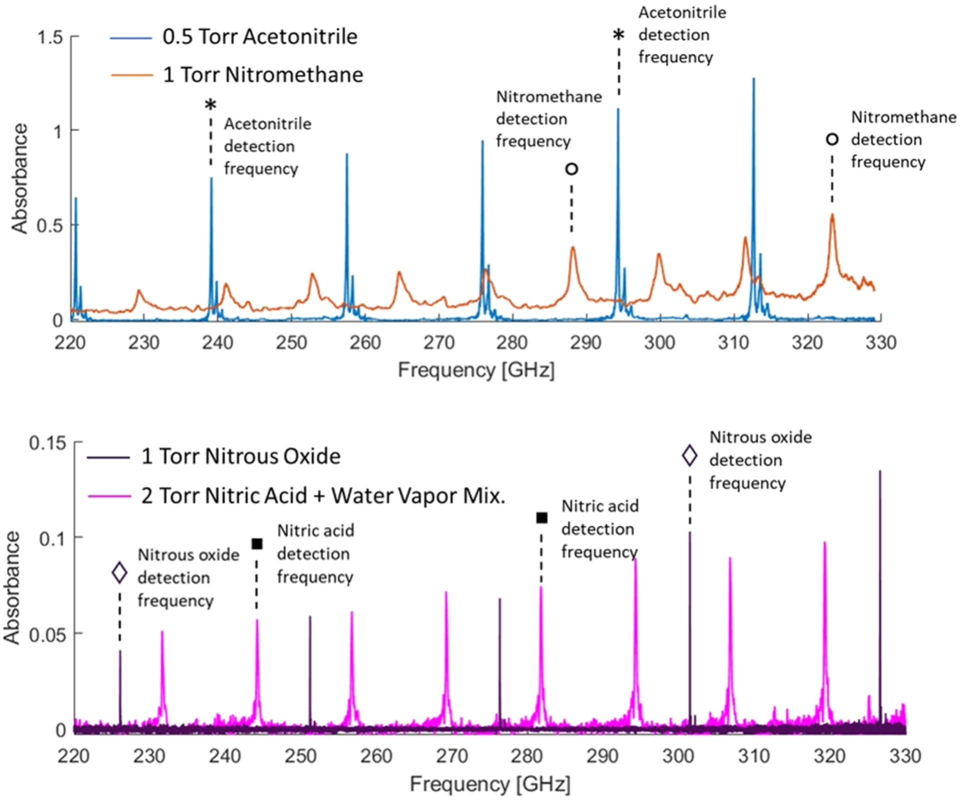

Fig. 11. Comparison of absorbance measurements for the four compounds of interest with recommended detection frequencies.

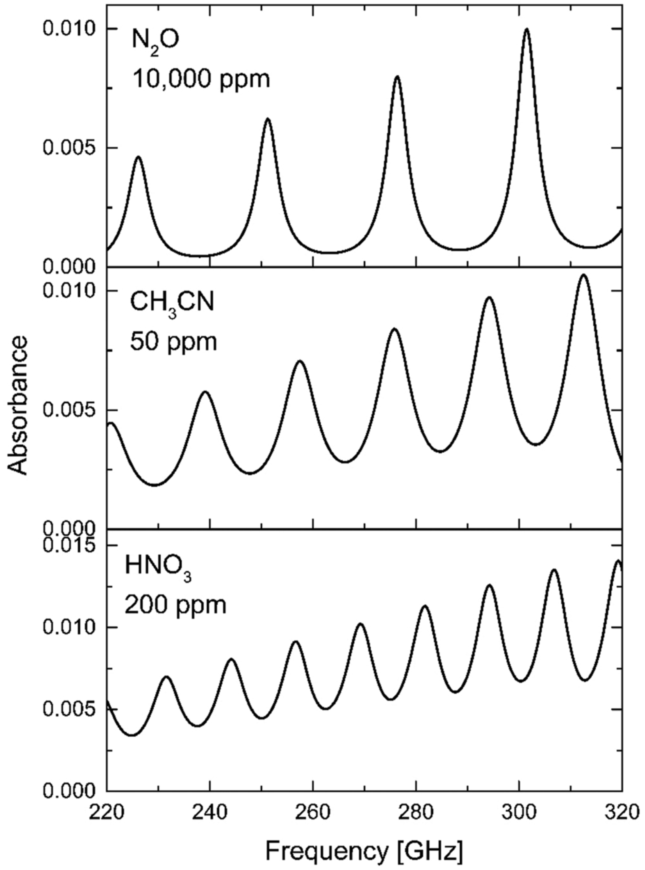

Fig. 12. Modeled absorbance for nitrous oxide (top), acetonitrile (middle), and nitric acid (bottom) in air at 1 atm. The concentrations given provide a signal-to-noise ratio of ten, assuming a noise floor of ± 0.001.

presence of small concentrations of nitromethane.

Detection limits for the four compounds of interest at the selected frequencies are estimated and provided in Table 1, based on an assumed absorbance noise floor of ± 0.001 and the measured spectral absorbance. The minimum detectible absorbance for the present experiments is in the range $A = \ln\left(\frac{I}{I_0}\right) = 0.001–0.003$, and averaging or filtering of the signals can be used to reduce this minimum detectible absorbance below this level. Detection limits for pure gases result from the measured absorbance levels in comparison to a noise floor of ± 0.001. The estimated detection limits for pure gases are in the range of 10^{12} to 10^{13} molecules/cm^3 per meter pathlength.

For estimation of detection limits for gases dilute in air at 1 atm, pressure-broadened spectra were modeled using extrapolated line broadening parameters [34–36]. Pressure-broadened spectra at 1 atm contain blending of features which makes species identification difficult but not impossible. For example, see the modeled spectra for three of the species of interest dilute in air at 1 atm in Fig. 12 which illustrates broad repeating features with line half widths of order of a GHz. For the target gases dilute in air, the detection limits are in the range of 5–1000 ppm per meter pathlength, which may allow application of absorption sensors in this frequency region for remote industrial gas monitoring. Note, that the larger species, acetonitrile, nitric acid, and nitromethane, provide significantly lower detection limits when dilute in air than the smaller nitrous oxide, due to the strength of the resulting pressure-broadened/blended features that contain many lines.

4. Conclusions

Gas sensing in the 220–330 GHz range based on rotational absorption spectroscopy has been demonstrated for four nitrogen-containing compounds of industrial relevance (nitrous oxide, acetonitrile, nitric acid, and nitromethane) using a microelectronics-based THz spectrometer. Spectral absorption at 297 K and pressures from 33.3 to 2133 Pa (0.25–16 Torr), where collisional line broadening plays a role, has been characterized. The spectra illustrate strong absorption features typically containing contributions from multiple rotational transitions in either vibrational ground states or low-lying bending states that allow for the selective measurement of these compounds with detection limits of 10^{12}-10^{13} molecules cm^{-3} per meter pathlength under pure conditions and 5–1000 ppm per meter pathlength for dilute gases in air at 1 atm. The demonstrated sensing method has sensitivity and potential for application to remote gas sensing in industrial applications where process and emission control over nitrogen-containing compounds is required.

CRediT authorship contribution statement

Timothy E. Rice: Conceptualization, Methodology, Software, Validation, Formal analysis, Investigation, Writing – original draft, Visualization. **M. Arshad Zahangir Chowdhury:** Methodology, Investigation. **Megan N. Powers:** Investigation. Muhammad Waleed Mansha: Methodology. **Ingrid Wilke:** Conceptualization, Writing – review & editing, Supervision. **Mona M. Hella:** Conceptualization, Supervision. **Matthew A. Oehlschlaeger:** Conceptualization, Writing – review & editing, Supervision, Project administration.

Declaration of Competing Interest

The authors declare the following financial interests/personal relationships which may be considered as potential competing interests: Matthew Oehlschlaeger reports financial support was provided by National Science Foundation. Matthew Oehlschlaeger reports a relationship with National Science Foundation that includes: funding grants.

Acknowledgement

This research was funded by the National Science Foundation of the United States under Grant CBET-1851291.

Appendix A. Supporting information

Supplementary data associated with this article can be found in the online version at doi:10.1016/j.snb.2022.132030.

References

[1] R.M. Smith, M.A. Arnold, Selectivity of terahertz gas-phase spectroscopy, Anal. Chem. 87 (2015) 10679–10683, https://doi.org/10.1021/acs.analchem.5b03028.

[2] Y.-D. Hsieh, S. Nakamura, D.G. Abdelsalam, T. Minamikawa, Y. Mizutani, H. Yamamoto, T. Iwata, F. Hindle, T. Yasui, Dynamic terahertz spectroscopy of gas molecules mixed with unwanted aerosol under atmospheric pressure using fibre-based asynchronous-optical-sampling terahertz time-domain spectroscopy, Sci. Rep. 6 (2016) 28114, https://doi.org/10.1038/srep28114.

[3] Y. Yang, A. Shutler, D. Grischkowsky, Measurement of the transmission of the atmosphere from 0.2 to 2 THz, Opt. Express 19 (2011) 8830–8838, https://doi.org/10.1364/OE.19.008830.

[4] S.L. Dexheimer, Terahertz Spectroscopy Principles and Applications, CRC Press, Boca Raton, 2008.

[5] A. Tekawade, T.E. Rice, M.A. Oehlschlaeger, M.W. Mansha, K. Wu, M.M. Hella, I. Wilke, Towards realization of quantitative atmospheric and industrial gas sensing using THz wave electronics, Appl. Phys. B 124 (2018) 105, https://doi.org/10.1007/s00340-018-6974-1.

[6] M.W. Mansha, K. Wu, T.E. Rice, M.A. Oehlschlaeger, I. Wilke, M.M. Hella, A 220–300 GHz Twin-FET detector for rotational spectroscopy of gas mixtures, IEEE Sens. J. 21 (2020) 4553–4562, https://doi.org/10.1109/JSEN.2020.3031838.

[7] T.E. Rice, M.W. Mansha, M.A.Z. Chowdhury, M.M. Hella, I. Wilke, M. A. Oehlschlaeger, VOC gas sensing via microelectronics-based absorption spectroscopy at 220–330 GHz, Appl. Phys. B 126 (2020) 152, https://doi.org/10.1007/s00340-020-07501-9.

[8] T.E. Rice, M.A.Z. Chowdhury, M.W. Mansha, M.M. Hella, I. Wilke, M. A. Oehlschlaeger, Halogenated hydrocarbon gas sensing by rotational absorption spectroscopy in the 220–330 GHz frequency range, Appl. Phys. B 127 (2021) 123, https://doi.org/10.1007/s00340-021-07667-w.

[9] M. Exter, C. Fattinger, D. Grischkowsky, Terahertz time-domain spectroscopy of water vapor, Opt. Lett. 14 (1989) 1128–1130, https://doi.org/10.1364/OL.14.001128.

[10] K. Schmalz, N. Rothbart, M.H. Eissa, J. Borngräber, D. Kissinger, H.-W. Hübers, Transmitters and receivers in SiGe BiCMOS technology for sensitive gas spectroscopy at 222–270 GHz, AIP Adv. 9 (2019), 015213, https://doi.org/10.1063/1.5066261.

[11] R. Han, Z. Hu, C. Wang, J. Holloway, X. Yi, M. Kim, J. Mawdsley, Filling the gap: silicon terahertz integrated circuits offer our best bet, IEEE Microw. Mag. 20 (2019) 80–93, https://doi.org/10.1109/MMM.2019.2891379.

[12] M.W. Mansha, K. Wu, T.E. Rice, M.A. Oehlschlaeger, M.M. Hella, I. Wilke, Detection of volatile organic compounds using a single transistor terahertz detector implemented in standard BiCMOS technology, IEEE Sens. (2019) 1–4, https://doi.org/10.1109/SENSORS43011.2019.8956555.

[13] N. Rothbart, O. Holz, R. Koczulla, K. Schmalz, H.W. Hübers, Analysis of human breath by millimeter-wave/terahertz spectroscopy, Sensors 19 (2019) 2719, https://doi.org/10.3390/s19122719.

[14] I.R. Medvedev, R. Schuefler, J. Thomas, O. Kenneth, H.-J. Nam, N. Sharma, Q. Zhong, D.J. Lary, P. Raskin, Analysis of exhaled human breath via terahertz molecular spectroscopy, 41st International Conference on Infrared, Millimeter, and Terahertz Waves (IRMMW-THz) (2016) 1–2. doi: 10.1109/IRMMW-THz.2016.7758450.

[15] D. Bigourd, A. Cuisset, F. Hindle, S. Matton, R. Bocquet, G. Mouret, F. Cazier, D. Dewaele, H. Nouali, Multiple component analysis of cigarette smoke using THz spectroscopy, comparison with standard chemical analytical methods, Appl. Phys. B 86 (2007) 579–586, https://doi.org/10.1007/s00340-006-2495-4.

[16] M. Naftaly, N. Vieweg, A. Deninger, Industrial applications of terahertz sensing: state of play, Sensors 19 (2019) 4203, https://doi.org/10.3390/s19194203.

[17] C.F. Neese, I.R. Medvedev, G.M. Plummer, A.J. Frank, C.D. Ball, F.C. De Lucia, Compact submillimeter/terahertz gas sensor with efficient gas collection, preconcentration, and ppt sensitivity, IEEE Sens. J. 12 (2012) 2565–2574, https://doi.org/10.1109/JSEN.2012.2195487.

[18] P. Ricaud, J.L. Attié, R. Chalinel, F. Pasternak, J. Léonard, I. Pison, E. Pattey, R. L. Thompson, Z. Zelinger, J. Lelieveld, J. Sciare, The monitoring nitrous oxide sources (MIN2OS) satellite project, Remote Sens. Environ. 266 (2021), 112688, https://doi.org/10.1016/j.rse.2021.112688.

[19] Environmental Protection Agency, Overview of Greenhouse Gases. 〈https://www.epa.gov/ghgemissions/overview-greenhouse-gases#nitrous-oxide〉, 2022 (accessed 03 March 2022).

[20] N.D.C. Allen, J.J. Harrison, P.F. Bernath, Acetonitrile (CH3CN) infrared absorption cross sections in the 3μm region, J. Quant. Spectrosc. Radiat. Transf. 112 (2011) 1961–1966, https://doi.org/10.1016/j.jqsrt.2011.04.001.

[21] J.A. de Gouw, C. Warneke, D.D. Parrish, J.S. Holloway, M. Trainer, F.C. Fehsenfeld, Emission sources and ocean uptake of acetonitrile (CH3CN) in the atmosphere, J. Geophys. Res 108 (2003) D11, https://doi.org/10.1029/2002jd002897.

[22] HIS Markit, Chemical Economics Handbook, 〈https://ihsmarkit.com/products/nitric-acid-chemical-economics-handbook.html〉, 2022 (accessed 03 March 2022).

[23] Environmental Protection Agency, What is Acid Rain?, 〈https://www.epa.gov/acidrain/what-acid-rain〉, 2022 (accessed 03 March 2022).

[24] E.J. Slingerland, E.G.E. Jahngen, T.M. Goyette, R.H. Giles, W.E. Nixon, Terahertz absorption spectra of nitromethane, J. Quant. Spectrosc. Radiat. Transf. 112 (2011) 2323–2329, https://doi.org/10.1016/j.jqsrt.2011.06.006.

[25] V. Ilyushin, Millimeter wave spectrum of nitromethane, J. Mol. Spectrosc. 345 (2018) 64–69, https://doi.org/10.1016/j.jms.2017.12.005.

[26] G.B. Taylor, Vapor pressure of aqueous solutions of nitric acid, Ind. Eng. Chem. 17 (1925) 633–635.

[27] B.A. Andreev, A.V. Burenin, E.N. Karyakin, A.F. Krupnov, S.M. Shapin, Submillimeter wave spectrum and molecular constants of N2O, J. Mol. Spectrosc. 62 (1976) 125–148, https://doi.org/10.1016/0022-2852(76)90344-1.

[28] H.M. Pickett, R.L. Poynter, E.A. Cohen, M.L. Delitsky, J.C. Pearson, H.S.P. Müller, Submillimeter, millimeter, and microwave spectral line catalog, J. Quant. Spectrosc. Radiat. Transf. 60 (1998) 883–890, https://doi.org/10.1016/S0022-4073(98)00091-0.

[29] D. Boucher, J. Burie, A. Bauer, A. Dubrulle, J. Demaison, Microwave spectra of molecules of astrophysical interest. XIX. methyl cyanide, J. Phys. Chem. Ref. Data 9 (1980) 659–720, https://doi.org/10.1063/1.555625.

[30] T. Shimanouchi, Tables of Molecular Vibrational Frequencies Consolidated Volume I, National Bureau of Standards, 1972, 1–160.

[31] D.J. Millen, J.R. Morton, The microwave spectrum of nitric acid, J. Chem. Soc. 307 (1960) 1523–1528.

[32] F. Rohart, Microwave spectrum of nitromethane internal rotation hamiltonian in the flow barrier case, J. Mol. Spectrosc. 57 (1975) 301–311, https://doi.org/10.1016/0022-2852(75)90033-8.

[33] C.M. Western, B.E. Billinghurst, Automatic and semi-automatic assignment and fitting of spectra with PGOPHER, Phys. Chem. Chem. Phys. 21 (2019) 13986–13999, https://doi.org/10.1039/C8CP06493H.

[34] E. Adkins, D.A. Long, A.J. Fleisher, J.T. Hodges, Near-infrared cavity ring-down spectroscopy measurements of nitrous oxide in the (4200)-(0000) and (5000)-(0000) bands, J. Quant. Spectrosc. Radiat. Transf. 262 (2021), 262107527, https://doi.org/10.1016/j.jqsrt.2021.107527.

[35] C.P. Rinsland, V. Malathy Devi, D. Chris Benner, T.A. Blake, R.L. Sams, L.R. Brown, I. Kleiner, A. Dehayem-Kamadjeu, H.S.P. Müller, R.R. Gamache, D.L. Niles, T. Masiello, Multispectrum analysis of the v4 band of CH3CN: positions, intensities, self- and N2-broadening, and pressure-induced shifts, J. Quant. Spectrosc. Radiat. Transf. 109 (2008) 974–994, https://doi.org/10.1016/j.jqsrt.2007.11.013.

[36] L. Zu, P.A. Hamilton, P.B. Davies, Pressure broadening and frequency measurements of nitric acid lines in the region, J. Quant. Spectrosc. Radiat. Transf. 73 (2002) 545–556, https://doi.org/10.1016/s0022-4073(01)00176-5.

Timothy E. Rice is a Ph.D. candidate in Aerospace Engineering at Rensselaer Polytechnic Institute. His research is in the area of gas sensor development using THz-wave absorption.

M. Arshad Chowdhury is a PhD candidate in Mechanical Engineering at Rensselaer Polytechnic Institute. His research focuses on spectroscopy and automated learning algorithms for gas sensing.

Megan N. Powers is an undergraduate researcher at Rensselaer Polytechnic Institute where she is pursuing a B.S. in Aeronautical Engineering and engaged in research on gas sensing.

Muhammad Waleed Mansha obtained a Ph.D. in Electrical Engineering from Rensselaer Polytechnic Institute in 2021. His research focuses on the development of THz electronic devices. He is currently a staff researcher at Nokia Bell Labs.

Ingrid Wilke obtained a Ph.D. in Physics from ETH Zurich in 1993. She has been on the faculty of Physics, Applied Physics, and Astronomy at Rensselaer Polytechnic Institute since 2002. Her research efforts are in the areas of THz spectroscopy, ultrafast spectroscopy, and applications of femtosecond laser pulses.

Mona M. Hella obtained a Ph.D. in Electrical Engineering from Ohio State University in 2001. She has been on the faculty of Electrical and Computer Systems Engineering at Rensselaer Polytechnic Institute since 2004. Her research focuses on millimeter wave and THz integrated circuits, high-speed circuits for wireless/optical transceivers, and biomedical and energy harvesting interface integrated circuits.

Matthew A. Oehlschlaeger obtained a Ph.D. in Mechanical Engineering from Stanford University in 2005. He has been on the faculty of Mechanical and Aerospace Engineering at Rensselaer Polytechnic Institute since 2006. His research focuses on sensors, spectroscopy, chemical kinetics, combustion, and energy.